Brownian Dynamics Simulation of DNA Fragments in Strong Electric Fields

Suzann Mazur and Stuart A. Allison*

Department of Chemistry, Georgia State University, Atlanta, Georgia 30303

Received: September 26, 1996; In Final Form: December 13, 1996[⊗]

Brownian dynamics simulation is used to study the transient deformation of semiflexible polyions (specifically a 194 bp DNA fragment) in time varying electric fields. The polyion is represented as a string of beads, and the interaction of the polyion with the electric field is accounted for by placing effective charges on the subunits. Charge polarization effects are included by adapting the model of Szabo, Haleem, and Eden (*J. Chem. Phys.* **1986**, *85*, 7422), which also accounts for the response time of the ion atmosphere to a time varying field. Simulation results are in qualitative agreement with transient electric dichroism experiments on short DNA fragment which exhibit "amplitude inversion". Amplitude inversion is a consequence of a bowing deformation which results from the electrophoretic migration of the polyion. The model studies also show that the bowing deformation can be eliminated by replacing a constant electric field pulse (of duration T) with a rapidly reversing square wave of period $2T'$, provided T' is short compared to the coil deformation time of the fragment but long compared to the ion atmosphere relaxation time.

Introduction

Methods that involve subjecting a macromolecule to an external field and then monitoring some response such as migration (electrophoresis) or orientation (dichroism or birefringence) are pervasive in science. In fact, more than half of the scientific publications in biochemistry depend to some degree on the application of electrophoretic or related electrokinetic methods.[1] In recent years, considerable attention has been given to field modulation techniques such as pulsed field gel electrophoresis (PFGE) which has made it possible to separate DNA molecules of more than 20 000 base pairs.[2,3] Field modulation in transient electric birefringence (TEB) or dichroism (TED) experiments have not been exploited to the extent they have in electrophoresis, but are also potentially powerful methods.[4,5] As pointed out by Oppermann,[4] unusual birefringence transients may be eliminated by modulating the applied electric fields with high-frequency ac fields. It has been argued that the simpler birefringence behavior at high-frequency ac fields is due to the elimination of effects such as polyion deformation.[4] Thus, field-modulated electric birefringence and dichroism may provide information about the unperturbed state of polyions in solution. To understand how field modulation might be useful in the study of DNA restriction fragments, it will be helpful to briefly review some important observations of TED and TEB studies under different conditions.

At very low field strengths (up to 1 kV/cm), the TED of DNA fragments is quite complicated,[5] which has been attributed to a permanent dipole moment that is comparable (at low external field) to the induced dipole moment. It has been proposed that this permanent dipole arises from DNA conformations that are bent[6] and/or asymmetric ligand or ion binding.[6−8] The moderate field strength regime, where the induced dipole or saturated induced dipole[9,10] evidently swamps out the contribution from the small permanent dipole moment, has been extensively studied[11−14] and is the best understood regime. The off-field TEB or TED decay of short DNA fragments consists of a large-amplitude component that decays exponentially with a lifetime that corresponds closely to end-over-end rotational diffusion and also a smaller amplitude component with a much shorter lifetime. Brownian dynamics simulations of discrete wormlike chains unperturbed by the external field have been carried out to understand these TEB/TED decays.[15,16] These studies have shown that the faster decay component is sensitive to bending flexibility and that the model that fits the experimental data best is a semiflexible chain with no permanent bends and a stiffness parameter appropriate for a wormlike chain with a persistence length of 50 nm.

Above a field strength of about 10 kV/cm, DNA fragments appear to be deformed by the electric field as evidenced by anomalous behavior of the TED lifetimes and amplitudes.[14] Since DNA absorbs UV light more strongly in the plane of the base pairs, which is roughly perpendicular to the helix axis, it usually exhibits negative dichroism. Under certain conditions, however, the TED starts off negative, as usual when the field is turned off, but rapidly increases and actually becomes positive before finally decaying to zero. Conditions that favor "amplitude inversion" are high field strength (above 10 kV/cm), monovalent salt concentrations above 5 mM (where the electric polarizability of the fragment is low), and DNA fragments that are about 200 bp in length.[17] The phenomenon of amplitude inversion appears to be closely associated with a bowing deformation of the fragment in the field direction as illustrated in Figure 1. At the moment the field is turned off, the average dichroism is negative since the plane of most of the base pairs is perpendicular to the field direction. Once the field is turned off, the field-induced deformation will relax and the chain will reorient. These processes occur on different time scales with the coil deformations occurring more quickly in the case of short DNA fragments. For a 194 bp fragment, for example, deformation/overall reorientation occur on the 0.3/3.0 μs time scale.[16] Hence, the first change in conformation that would be expected to occur for the chain depicted in Figure 1 is that it would straighten out in about 0.3 μs and give rise to a positive dichroism. At longer times, the chain would tumble and the dichroism would decay to zero. This example provides a simple physical interpretation of the phenomenon. Using the technique of Brownian dynamics simulation, Elvingson[18] provided an explanation for the bowing deformation and showed it led to amplitude inversion under certain conditions. In the presence of a constant external field, DNA translates through the solution since it is a polyanion. Intrasubunit hydrodynamic interaction

[⊗] Abstract published in *Advance ACS Abstracts,* February 1, 1997.

S1089-5647(96)02968-9 CCC: $14.00

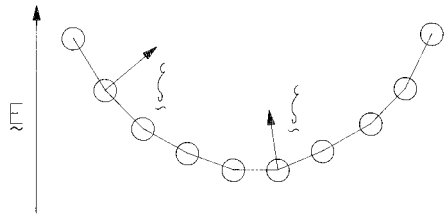

Figure 1. Schematic of a chain in an external electric field. In a constant field, a negatively charged chain bows as indicated in order to reduce frictional drag. The principal normal is indicated by ζ.

forces the chain to adopt a bowed conformation. In preliminary Brownian dynamics simulations, we have shown that amplitude inversion can occur for model parameters that are reasonable for DNA.[19] The objective of this work is to look more closely at the behavior of DNA fragments in high fields and show how a rapidly reversing (square wave) electric field can largely eliminate the deformation of the chain. In the next section, we briefly describe the discrete wormlike chain model used in the Brownian dynamics simulation. The most difficult aspect of this problem to deal with involves modeling the interaction of a polyion with an external electric field. The external electric field interacts with and polarizes the ion atmosphere in a complex way that involves the coupled dynamics of macromolecule, co- and counterions, and solvent. The treatment that accounts most completely for all the interactions present in electric polarization of charged cylinders is that of Fixman and Jagannathan.[20] There is an extensive literature on the subject summarized in a review by Charney,[21] which refers to many additional theories or models of electric polarization of macromolecules. Basically, what we need for the present work is a model of electric polarization that is realistic enough to account for the effect in a way that is qualitatively correct yet simple enough to be adaptable to the Brownian dynamics simulation of semiflexible wormlike chains. The polarization model we shall use is an adaption of the Szabo, Haleem, and Eden model for rodlike polyions[22] which shall hereafter be referred to as the single lifetime (SL) model. This model accounts for the coupled dynamics of the rotating polyion and ion atmosphere through a single ion atmosphere relaxation time, τ_I, and an electric polarizability, α. As discussed in a later section, it is straightforward to formulate a Brownian dynamics alogrithm based on the SL model that accounts for the instantaneous dipole moment of the polyion. From this dipole moment, we can place polarization charges, q_j', on various subunits of the chain. Since polyions carry net charges and the sum of the polarization charges is zero, it will also be necessary to put constant charges, q_{eff}, on each of the subunits of the chain. The net subunit charges then couple the polyion dynamics to the external field. This procedure accounts implicitly for the ion atmosphere dynamics of the polyion.

Methods

Discrete Wormlike Chain Model. Detailed descriptions of the discrete wormlike chain model and the approach used to parametrize them for light scattering[23] and electric birefringence/dichroism[16] are given elsewhere. Briefly, a DNA fragment is modeled as a string of N identical beads of radius a held together by bending (U^b) and stretching (U^s) potentials

$$\beta U^b = \frac{g}{2}\sum_{j=2}^{N-2}\theta_j^2 \tag{1}$$

$$\beta U^s = \frac{c}{2}\sum_{j=1}^{N-1}\left(\frac{b_j - b_0}{b_0}\right) \tag{2}$$

where $\beta = 1/k_BT$, g and c are dimensionless force constants for bending and stretching, θ_j is the angle between virtual bonds j and $j+1$ (the jth virtual bond vector, $\mathbf{b}_j$, is defined as $\mathbf{r}_{j+1} - \mathbf{r}_j$ where $\mathbf{r}_j$ is the instantaneous position of subunit j), $b_j = |\mathbf{b}_j|$, and b_0 corresponds to the minimum in the stretching potential. Overall, five parameters need to be specified to fully define a wormlike chain used in this work: N, c, a, b_0, and g. As in previous work, N and c are simply chosen, and then a, b_0, and g are determined by an equilibrium ensemble simulation (EES) method.[16]

In the EES method one starts by determining the eigenvalues of the rotational diffusion tensor averaged over an ensemble of wormlike chains frozen in equilibrium conformations that are characterized by contour length L, persistence length P, and diameter d. For example, DNA has a persistence length of about 50 nm under typical salt conditions[16] and a diameter of 1.2 nm.[24] The contour length is easily estimated once we know the number of base pairs in the fragment since the length per base pair is 0.34 nm. In the next step of the EES approach, an iterative approach is used to find an "equivalent" chain that has the same ensemble-averaged rotational eigenvalues as the corresponding wormlike chain.[16] Basically, what we are attempting to do here is find a "coarse-grained" chain that exhibits the same rotationally diffusive behavior as the actual DNA fragment we are trying to mimic. In previous work on short DNA fragments in moderate fields, the electric dichroism/birefringence decays were analyzed using CONTIN[25] to determine the amplitudes and lifetimes of the two longest decay modes.[16] For a 194 bp fragment with $P = 50$ nm, an equivalent chain of 10 beads was found to have the same amplitudes and lifetimes of the lowest two modes as a more detailed model consisting of touching beads (Table II of ref 16). Furthermore, almost the entire decay amplitude occurred in the two longest lifetime modes. On this basis, we concluded that the equivalent chain is detailed enough to reproduce the electric birefringence/dichroism decay of the actual DNA fragment. In the present study, much of the work reported is on a 194 bp DNA fragment with $P = 50$ nm at 294 K. The parameters for the corresponding equivalent chain are $N = 10$, $c = 400$, $a = 1.93$ nm, $b_0 = 7.33$ nm, and $g = 6.51$.

Electrostatic Interaction. As discussed in the Introduction, the electrostatic interaction of the polyion with the external field is a complex problem since it involves not only the polyion itself but the surrounding ion atmosphere and solvent as well. A detailed account of this is beyond the scope of this work. The approach used here is to simply place carefully chosen charges on the subunit, and it is then these charges which interact with the external electric field. Despite its shortcomings, this model should account qualitatively for the interaction of the polyion with the external field.

If q_j is the charge on subunit j (in protonic units), then we write

$$q_j = q_{\text{eff}} + q_j' \tag{3}$$

where q_{eff} is an effective subunit charge in the limit the external field, $\mathbf{E}$, goes to zero, and q_j' represents the subunit polarization charge due to the external field. For the example of a 194 bp DNA fragment modeled as a 10 subunit chain, we can take $q_{\text{eff}} = 19.4q_{\text{bp}}$ where q_{bp} is an effective charge per base pair. At first glance, it might appear that a charge of $q_{\text{bp}} = -2$ would be appropriate due to deprotonation of the two phosphate moieties, but this ignores the ion atmosphere which would reduce the absolute value of q_{bp}. Indeed, if the ion atmosphere moved with polyion as a rigid body (which it does not), the effective base pair charge should equal zero. A more reasonable choice would be to assume $q_{\text{bp}} = -0.48$ since this corresponds to 76% neutralization of the DNA phosphate charges by

counterion condensation.[26] To the best of our knowledge, the only relevant experimental measurement of effective charge comes from the work of Smith and Bendich,[27] who studied the distortion of high molecular weight plasmid DNA's in electric fields that are immobilized by agarose fibers, and they inferred an effective charge of -15 per persistence length, which corresponds to $q_{bp} = -0.10$. We set $q_{bp} = -0.24$ as a compromise between the counterion condensation estimate and the Smith−Bendich value. As discussed previously,[19] this choice does lead to "amplitude inversion" of the birefringence decay at a field strength of 25 kV/cm provided the electric polarizability is lower than about 0.25×10^{-16} cm^3. From the known salt dependence of the electric polarizability of DNA fragments of this size, we can interpret this as corresponding to the onset of amplitude inversion above a monovalent salt concentration of 12.5 mM, which is qualitatively consistent with experiment.

For the polarization charges, q_j', we turn to an adaptation of the single lifetime (SL) model of Szabo, Haleem, and Eden[22] for the electric polarization of a rodlike polyion. In this model, an induced dipole moment, **p**, develops along a single axis of the polyion, which in the original work was assumed to coincide with the long axis of the rod. In the present work, we shall assume this axis lies along the end-to-end vector of the wormlike chain. Define this axis as the *x*-axis in a body-fixed reference frame of the polyion (Σ_p). The instantaneous dipole moment (along *x* of Σ_p) is related to the polarization charge, ne_0, and displacement vector between centers of positive and negative charge, $\delta(t)$, by

$$p(t) = ne_0\delta(t) \tag{4}$$

where $e_0 = 4.8 \times 10^{-10}$ esu and *n* is the number of ionized groups on the polyion. The total potential energy of the macroion can be written[22]

$$V(\theta, \delta) = (1/2\alpha)n^2e_0^2\delta^2 - ne_0\delta E\cos\theta \tag{5}$$

where α is the polyion polarizability, *E* is the external field strength, and θ is the instantaneous angle between **E** and the polyion axis.

It is straightforward to mimic the dynamic behavior of $\delta(t)$ using a simple Brownian dynamics protocol

$$\delta(t+\delta t) = \delta(t) + \omega(\Delta t) + v_d(t)\Delta t \tag{6}$$

where ω represents a stochastic displacement and v_d a "drift" velocity of the ion atmosphere (along *x* of Σ_p). The mean of ω is zero, and its variance is

$$\langle\omega^2(\Delta t)\rangle = 2D_I\Delta t \tag{7}$$

where brackets denote a time average and D_I is the ion atmosphere diffusion constant. We can also write

$$v_d(t) = -\beta D_I\frac{dV}{d\delta} = -\beta D_I\left[\frac{n^2e_0^2\delta(t)}{\alpha} - ne_0E(t)\cos\theta(t)\right] \tag{8}$$

Combining this with eq 6 gives

$$\delta(t+\Delta t) = \left(1 - \frac{\Delta t}{\tau_I}\right)\delta(t) + \omega(t) + \beta\Delta t ne_0D_IE(t)\cos\theta(t) \tag{9}$$

where

$$\tau_I = \alpha k_BT/n^2e_0^2D_I \tag{10}$$

is a single relaxation time of the ion atmosphere. This model assumes fluctuations in the root-mean-square (rms) dipole decay exponentially. The work of Vaughan and co-workers[28] shows that a large-amplitude component of the dipole does decay with a characteristic lifetime that is consistent with the SL model. In ref 22, a τ_I of 120 ns was found to reproduce the reverse pulse TEB of a 124 bp DNA fragment. Multiplying eq 9 by ne_0 and using eq 4 yields

$$p(t+\delta t) = (1 - \Delta t/\tau_I)p(t) + ne_0\omega(t) + \beta\Delta t(ne_0)^2D_IE(t)\cos\theta(t) \tag{11}$$

Equation 11 leads to more recognizable relationships under special conditions. For example, assume that τ_I is much smaller than the end-over-end tumbling time of the polyion. If eq 11 is averaged over times long compared to τ_I but short compared to end-over-end tumbling time (variation in cos $\theta(t)$), then

$$\langle p(t)\rangle = \alpha E(t)\cos\theta(t) \tag{12}$$

In the present work, the instantaneous dipole moment given by eq 11 is reproduced by placing polarization charges, $\pm q_{pol}(t)$, on subunits *N* and 1, respectively. Neglecting fluctuations in the end-to-end distance and replacing the instantaneous end-to-end displacement, $R(t)$, with the equilibrium end-to-end displacement, $\langle R^2\rangle^{1/2}$, we can write

$$p(t) = e_0q_{pol}(t)\langle R^2\rangle^{1/2} \tag{13}$$

and from eq 11

$$q_{pol}(t+\Delta t) = \left(1 - \frac{\Delta t}{\tau_I}\right)q_{pol}(t) + \epsilon(t) + \frac{\alpha\Delta tE(t)\cos\theta(t)}{e_0\langle R^2\rangle^{1/2}\tau_I} \tag{14}$$

where $\langle\epsilon(t)\rangle = 0$ and

$$\langle\epsilon(t)^2\rangle = 2D^*\Delta t \tag{15}$$

$$D^* = \alpha k_BT/e_0^2\langle R^2\rangle\tau_I \tag{16}$$

Equation 14 provides a simple means of incrementimg the polarization charges on the end subunits. Note that updating q_{pol} depends on the instantaneous field, orientation of the end-to-end vector with respect to **E**, and the SL model parameters α and τ_I. Despite some obvious shortcomings (such as assuming a single ion atmosphere relaxation time, assuming our nonlinear polyion polarizes along the end-to-end vector with constant polarizability that is independent of chain conformation, placing polarization charges on only the end subunits, and replacing $R(t)$ with $\langle R^2\rangle^{1/2}$), this strategy should account for the dynamic interaction of the polyion with an external field in a qualitatively reasonable manner. In addition, it is simple enough to be incorporated directly into existing Brownian dynamics simulation algorithms.

Brownian Dynamics. The Brownian dynamics algorithm of Ermak and McCammon[29] is used to generate the time evolution of model chains. Let $\mathbf{r}_i^0$ denote the position of subunit *i* at the start of a dynamics step of duration Δt. Its position after the dynamics step is given by

$$\mathbf{r}_i = \mathbf{r}_i^0 + \beta\Delta t\sum_{j=1}^{N}\boldsymbol{D}_{ij}^0\cdot\mathbf{F}_j^0 + \mathbf{S}_i(\Delta t) \tag{17}$$

where $\mathbf{F}_j^0$ is the initial direct force on subunit *j*, $\mathbf{S}_i$ is a vector

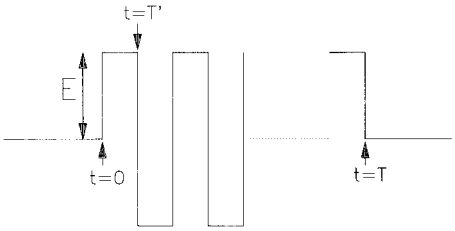

Figure 2. Applied electric field versus *t*. A field of strength *E* is turned on at $t = 0$ and off at $t = T$. At times T', $2T'$, $3T'$, etc., the field is reversed.

of Gaussian random numbers of zero mean and variance covariance

$$\langle \mathbf{S}_i \mathbf{S}_j \rangle = 2\boldsymbol{D}_{ij}^{\,0}\Delta t \tag{18}$$

and $\mathbf{D}_{ij}^0$ is the configuration-dependent hydrodynamic interaction tensor between subunits *i* and *j*. The zero superscript in the above two equations denotes the value of the quantity at the start of the dynamics step. In this work, the Rotne−Prager tensors are used for $\mathbf{D}_{ij}$.[30] For $i = j$,

$$\boldsymbol{D}_{ii} = \frac{k_B T}{6\pi\eta a}\boldsymbol{I} \tag{19}$$

where *a* is the (spherical) subunit radius, η is the solvent viscosity, and $\boldsymbol{I}$ is the 3×3 identity tensor. For different but nonoverlapping subunits,

$$\boldsymbol{D}_{ij} = \frac{k_B T}{8\pi\eta r_{ij}}\left[\boldsymbol{I} + \frac{\mathbf{r}_{ij}\mathbf{r}_{ij}}{r_{ij}^{\,2}} + \left(\frac{2a^2}{r_{ij}^{\,2}}\right)\left(\frac{1}{3}\boldsymbol{I} - \frac{\mathbf{r}_{ij}\mathbf{r}_{ij}}{r_{ij}^{\,2}}\right)\right] \tag{20}$$

where $\mathbf{r}_{ij} = \mathbf{r}_i - \mathbf{r}_j$ and $r_{ij} = |\mathbf{r}_{ij}|$. For overlapping subunits ($r_{ij} < 2a$)

$$\boldsymbol{D}_{ij} = \frac{k_B T}{6\pi\eta a}\left[\left(1 - \frac{9r_{ij}}{32a}\right)\boldsymbol{I} + \frac{3\mathbf{r}_{ij}\mathbf{r}_{ij}}{32ar_{ij}}\right] \tag{21}$$

The direct forces appearing in eq 17 arise from intramolecular stretching and bending forces as well as the interaction of the charged subunits with the external electric field,

$$\mathbf{F}_j = -\nabla_j(U^b + U^s) - q_j e_0 \mathbf{E}(t) \tag{22}$$

where ∇_j denotes gradient with respect to $\mathbf{r}_j$ and the subunit charge (in units of e_0) is given by eq 3. The charge−charge interactions are left out of $\mathbf{F}_j$. In the absence of an external field, they enter indirectly through the bending force constant, *g*, via the electrostatic persistence length.[31−33] The polarization charges on the end subunits are expected to be effectively screened by intervening ions. The field modulated electric field, $\mathbf{E}(t)$, is turned on with magnitude *E* at the start of a Brownian dynamics trajectory ($t = 0$) and is directed along the *z* axis of the lab frame. As shown in Figure 2, the applied field is a square wave that switches between $\pm E$ after time delays of duration T' and is finally turned off at time *T*.

Averages. A Brownian dynamics simulation consists of between 800 and 1000 independent trajectories of total duration $2T$, and chains are initially selected from an equilibrium ensemble.[34] For a 194 bp DNA chain the end-over-end tumbling time is about 3.5 μs.[16] Setting $T = 8$ μs ensures that the chains have almost achieved steady state orientation when the field is turned off ($t = 8$ μs) and have returned to an isotropic equilibrium distribution when the trajectory is ended ($t = 16$ μs). From this ensemble of trajectories, a reduced birefringence/dichroism is computed from

$$\Delta n(t) = (N-1)^{-1}\sum_{j=1}^{N-1}\langle z_{ij+1}^{\,2}(t) - x_{jj+1}^{\,2}(t)\rangle \tag{23}$$

where $z_{jj+1}(t)/x_{jj+1}(t)$ is the projection of the *j*th virtual bond along the *z*/*x* direction in the lab frame at time *t* and brackets denote an average over all trajectories. The actual dichroism, $\Delta A(t)$, is related to $\Delta n(t)$ by[16]

$$\Delta A(t) = (N-1)cl(a_{\parallel} - a_{\perp})\Delta n(t) \tag{24}$$

where *c* is the concentration of macromolecules, *l* is the path length of the cell, and $a_{\parallel} - a_{\perp}$ is the difference in absorption cross section parallel and perpendicular to the bond axis. Since this difference is negative for DNA, the sign of ΔA and Δn will be different. For short rodlike DNA's, ΔA will be negative in a constant external field. Likewise, transient birefringence decay can be related to $\Delta n(t)$ by a relation similar to eq 24.

In earlier work, we attributed amplitude inversion to a bowing of the DNA fragment.[19] To illustrate this more directly, additional averages are computed in the present work. The local unit tanget vector at the position of virtual bond *j* is simply

$$\mathbf{t}_j = (\mathbf{r}_{j+1} - \mathbf{r}_j)/b_j \tag{25}$$

where $b_j = |\mathbf{r}_{j+1} - \mathbf{r}_j|$ is the length of virtual bond *j*. For a continuous wormlike chain with contour point *s* varying from 0 to *L* where *L* is the contour length of the chain, we can make use of the Frenet formula[35]

$$\mathrm{d}\mathbf{t}(s)/\mathrm{d}s = \kappa(s)\,\boldsymbol{\zeta}(s) \tag{26}$$

where κ is the local "curvature" and $\boldsymbol{\zeta}$ is a unit vector called the "principal normal". Physically, $\kappa(s)$ corresponds to the reciprocal of the radius of curvature at *s*. For the chain depicted in Figure 1, we would expect κ to be larger in the center of the chain than at the ends. Also, $\boldsymbol{\zeta}$ points in the direction of the change of $\mathbf{t}$ as one moves along the contour of the chain. From Figure 1, we expect $\boldsymbol{\zeta}$ to be nearly collinear with the field (*z*) direction near the chain center but almost orthogonal at the ends. For a chain that is unbowed in the electric field, we would expect the ensemble average of $\kappa(s)$ to be nearly constant and the ensemble average of $\zeta_z(s)$ to be zero. We can discritize eq 26 by defining

$$\kappa_j\boldsymbol{\zeta}_j = \frac{2(\mathbf{t}_j - \mathbf{t}_{j-1})}{b_j + b_{j-1}} \tag{27}$$

Now κ_j is just the length of the vector on the right-hand side of eq 27 so it along with the unit vector $\boldsymbol{\zeta}_j$ are readily computed.

Results

We shall focus on a 194 bp DNA fragment with a persistence length of 50 nm modeled as a string of 10 beads ($a = 1.93$ nm, $b_0 = 7.3$ nm, $c = 400$, $g = 6.51$) placed in a transient electric field with $E = 25$ kV/cm with a net "on time" of $T = 8$ μs. Also, the subunit charge, q_{eff}, is set to -0.24 (in units of e_0) throughout. A total of 1000 trajectories are carried out for each simulation, and each trajectory consists of 16 000 dynamics steps with a time delay (Δt) of 1 ns. The main quantities that shall be varied are the field reversal time, T', molecular polarizability, α, and ion atmosphere relaxation time, τ_I.

To illustrate amplitude inversion and correlate this to a bowing deformation of the chain, set $T' = T$ (corresponding to a constant dc field of 8 μs duration) and $\tau_I = 1$ ns (corresponding to an ion atmosphere that polarizes instantly to an external field)

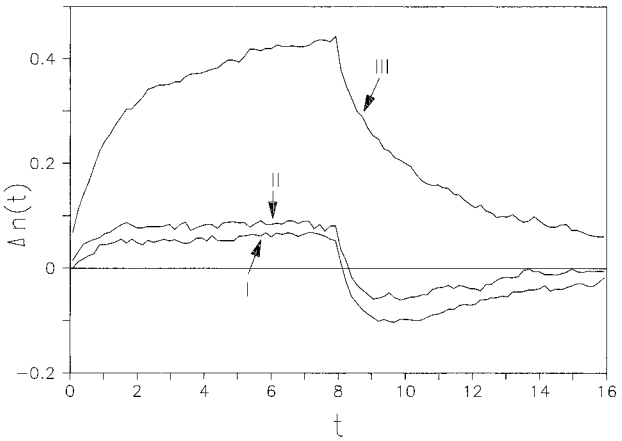

Figure 3. $\Delta n(t)$ versus t for variable α. For cases I, II, and III, α = 0.0, 0.25×10^{-16}, and 1.00×10^{-16} cm^3, respectively. There is no field reversal ($T = T'$), $E = 25$ kV/cm, and $\tau_I = 1$ ns. The time scale of the is abscissa is in microseconds.

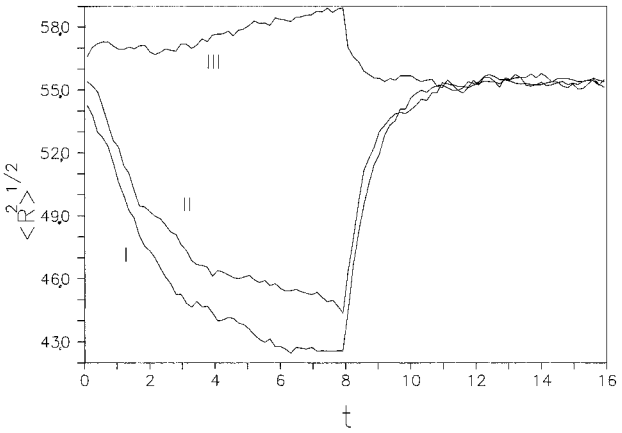

Figure 4. $\langle R^2\rangle^{1/2}$ versus t for variable α. Conditions are the same as in Figure 3. $\langle R^2\rangle^{1/2}$ is in nm.

but vary α from 0 to 1.0×10^{-16} cm^3. These polarizabilities are in the experimental range for fragments of this size.[17] Plotted in Figure 3 is $\Delta n(t)$ vs t for α = 0.0, 0.25×10^{-16}, and 1.00×10^{-16} cm^3. The curve with $\alpha = 1 \times 10^{-16}$ cm^3 exhibits typical birefringence/dichroism behavior, but the remaining two cases exhibit amplitude inversion after the field is turned off at 8 μs. The amplitude of Δn in the first part of the simulation increases as α increases since chains with larger α are more effectively oriented in an external field. It may appear somewhat surprising that the simulation with α = 0 has a measurable $\Delta n(t)$ at all since there is no polarization charge to help orient the chain. As the following analysis shows, however, there is substantial deformation of the chain, and this deformation is responsible for the nonvanishing Δn at low α. Plotted in Figure 4 are the ensemble average rms end-to-end distances vs time for the three polarizabilities. With the largest α, the chains are actually extended slightly, which is what would be expected for a polyion aligned along the external field direction with polarized charges of opposite sign placed on its ends. The other two cases, however, are actually compressed, which is consistent with a bowing of the chain as shown in Figure 1. As discussed previously,[18,19] this bowing is a consequence of the translation of the polyion in an external field. As it translates, intramolecular hydrodynamic interaction forces the chain to adopt a bowed conformation which reduces frictional drag. Setting $q_{\text{eff}} = 0$ or neglecting hydrodynamic interaction ($\mathbf{D}_{ij} = 0$ for $i \neq j$ in eqs 17 and 18) eliminates bowing. To show that the chain bows at its center and that the direction of bowing has the same sense as shown in Figure 1, the average z component of the principal normal (midchain) is plotted in

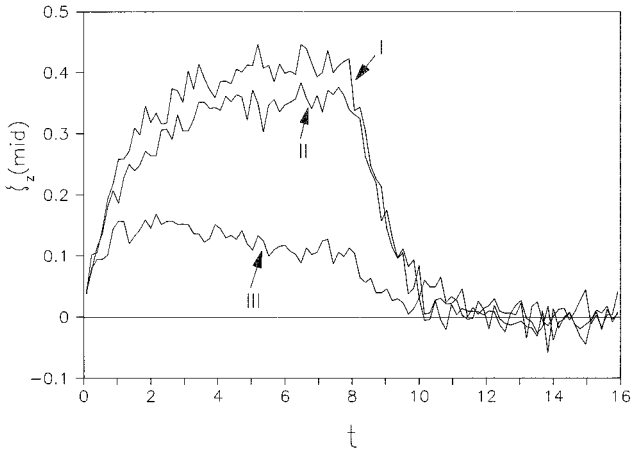

Figure 5. ζ_z(mid) versus t for variable α. Conditions are the same as in Figure 3.

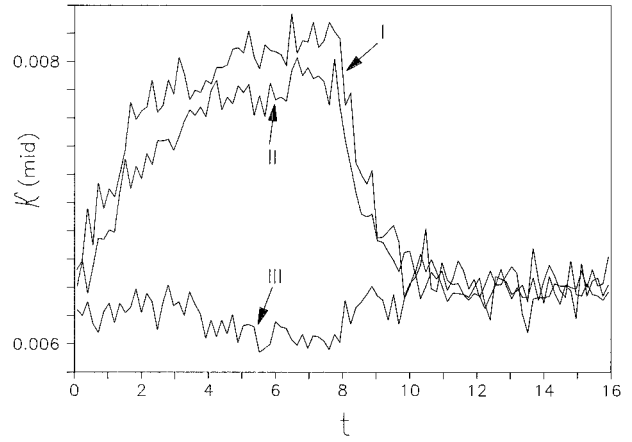

Figure 6. κ(mid) versus t for variable α. Conditions are the same as in Figure 3. κ is in nm^{-1}.

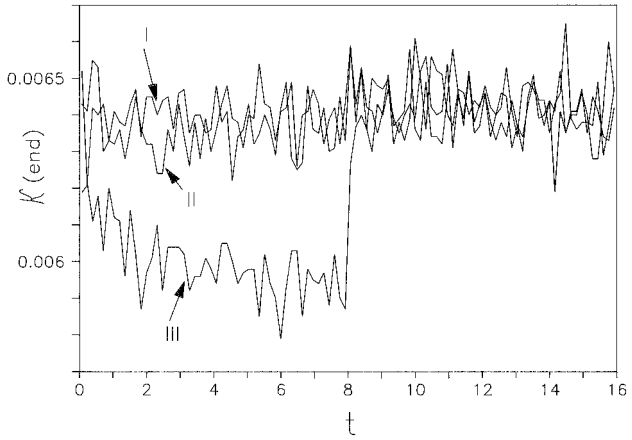

Figure 7. κ(end) versus t for variable α. Conditions are the same as in Figure 3.

Figure 5. Not only do the two lowest α cases show a positive $\langle\zeta_z(\text{mid})\rangle$ but so does $\alpha = 1 \times 10^{-16}$ cm^3 although it is substantially smaller. There are evidently two processes occurring simultaneously that deform the polyion: charge polarization tends to stretch the chain out, and electrophoretic translation tends to force it into a bowed conformation. At the chain ends, there turns out to be little if any correlation of the principal normal and the field direction. The dependence of curvature, κ, on time is plotted in Figures 6 (mid chain) and 7 (end chain). At low α, κ is unaffected or only slightly affected by an external field at the chain ends, but in the middle it is increased substantially. This is consistent with a kinking of the polyion at its center. The curvature in the high-polarizability

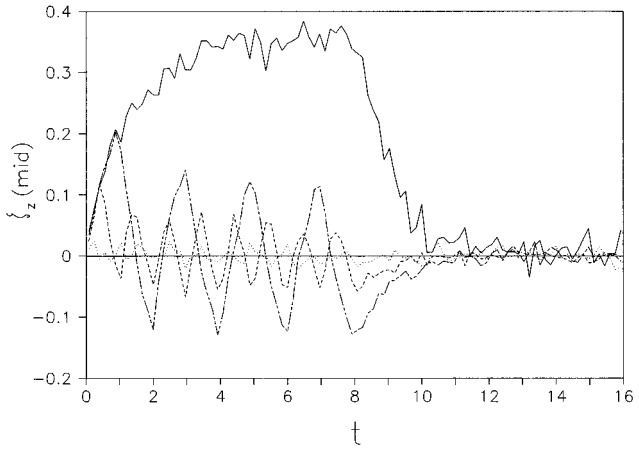

Figure 8. ζ_z(mid) versus t for variable T'. In all cases, $\alpha = 0.25 \times 10^{-16}$ cm^3, $E = 25$ kV/cm, and $\tau_I = 1$ ns. Dotted, dashed, dotted-dashed, and solid lines correspond to $T' = 100$, 500, 1000, and 8000 ns, respectively. The time scale for the abscissa is in microseconds.

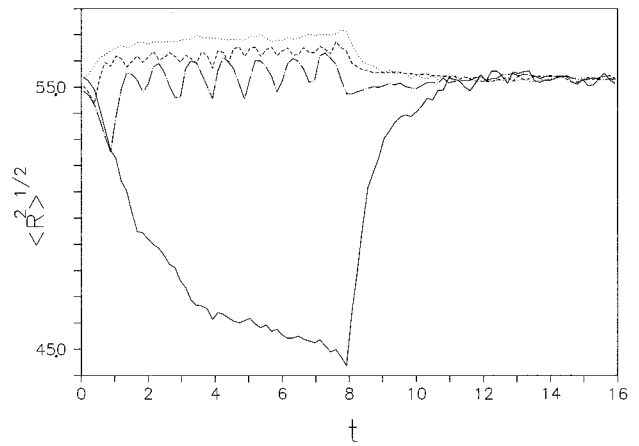

Figure 9. $\langle R^2 \rangle^{1/2}$ versus t for variable T'. Conditions are the same as in Figure 8.

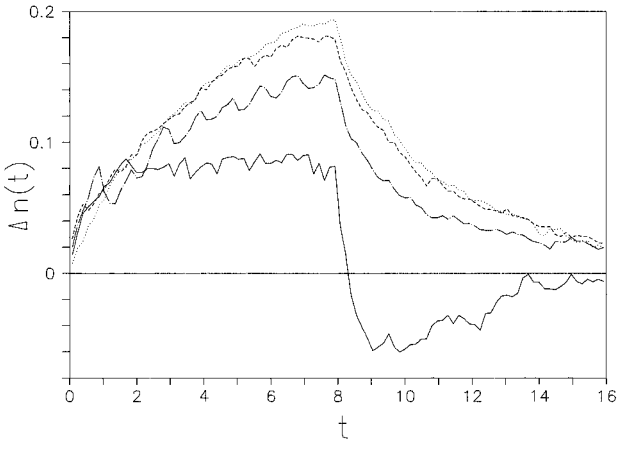

Figure 10. $\Delta n(t)$ versus t for variable T'. Conditions are the same as in Figure 8.

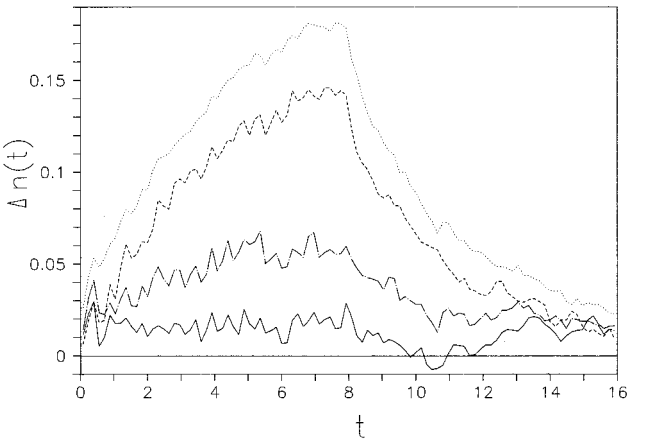

Figure 11. $\Delta n(t)$ versus t (in μs) for variable τ_I. In all cases, $\alpha = 0.25 \times 10^{-16}$ cm^3, $E = 25$ kV/cm, and $T' = 500$ ns. Dotted, dashed, dotted-dashed, and solid lines correspond to $\tau_I = 1$, 50, 200, and 500 ns, respectively.

case actually decreases slightly in an external field (consistent with stretching the fragment out), but there is not much variation in κ along the chain.

The three simulations discussed in the previous paragraph clearly exhibit field-induced deformation of the wormlike chain from its equilibrium conformation. We would now like to show how a rapidly reversing dc field can eliminate some of this deformation. The translation of the polyion should reverse if the field is reversed. If the field is reversed on a time scale that is fast compared to the internal bending times of the chain (several tenths of a microsecond for 194 bp DNA with $P = 50$ nm), the bowing deformations induced by the translation of the polyion should be eliminated. We shall set $\alpha = 0.25 \times 10^{-16}$ cm^3 and $\tau_I = 1$ ns and allow T' to vary. Other parameters are the same as before.

Shown in Figure 8 is the time dependence of $\langle \zeta_z(\text{mid}) \rangle$ with variable T' along with the steady state simulation considered previously. For $T' = 100$ ns (and also $T' = 200$ ns, which is not shown), the reversing field has entirely eliminated the bowing of the polyion. Even for $T' = 500$ ns, the bowing is largely eliminated although the spikes which are seen at 500 ns intervals indicate that partial bowing of the chains occur before the field is reversed. The effect is more striking for $T' = 1000$ ns. Figure 9 shows the corresponding behavior of $\langle R^2 \rangle^{1/2}$. It is worth noting that although a rapidly reversing field eliminates bowing, an increase in the end-to-end distance occurs which can be attributed to a stretching of the chain which occurs because of charge polarization. In other words, the deformation of the chain is partially but not completely eliminated by rapidly reversing the electric field. The behavior of the induced birefringence/dichroism is shown in Figure 10. Even a field reversal time as slow as 1 μs eliminates amplitude inversion. For T' shorter than about 0.5 μs, $\Delta n(t)$ becomes independent of the field reversal time. As discussed elsewhere,[36] the bowing deformation time should correspond to the longest bending lifetime of the chain.[37] For a chain of this length and stiffness, this corresponds to 0.5 μs to a reasonable approximation.

To this point, we have not accounted for the response time of the ion atmosphere to the external field other than assuming it is instantaneous ($\tau_I = 1$ ns). Brownian dynamics simulations on a rodlike polyion corresponding to a 40 bp DNA fragment exhibited a rise time of the induced dipole of about 19 ns.[38] Szabo et al.[22] fitted their reverse pulse TEB decay of a 124 bp DNA with a model of a rodlike polyion choosing $\tau_I = 117$ ns. From the theory of Vaughan and co-workers,[28,39] τ_I should vary roughly with the first power of the length, which leads us to anticipate $\tau_I \approx 150-200$ ns for a 194 bp DNA.

Shown in Figure 11 is $\Delta n(t)$ for $T' = 500$ ns and $\tau_I = 1$, 50, 200, and 500 ns. As τ_I increases, the principal effect on the TEB or TED appears to be a reduction in the steady state magnitude of the TEB or TED. This reduction occurs because the induced dipole moment develops more slowly as τ_I increases, and consequently there is less orientation of the polyion along the external field before it is reversed. From Figure 11, we can conclude that the magnitude of the TEB or TED becomes small when the field reversal time, T', is comparable to or smaller than τ_I. This conclusion is confirmed by additional studies with T' reduced to 100 ns (results not shown). Shown

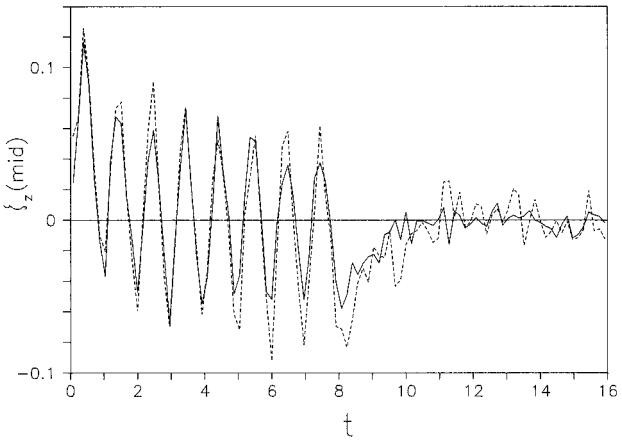

Figure 12. ζ_z(mid) versus t (in μs) for different τ_I. $\alpha = 0.25 \times 10^{-16}$ cm^3, $E = 25$ kV/cm, $T' = 500$ ns, and $\tau_I = 1$ ns (dotted line) and 500 ns (solid line).

in Figure 12 is the time dependence of ζ_z(mid) for $\tau_I = 1$ and 500 ns with a field reversal time of 500 ns. Bowing is expected to depend primarily on the effective subunit charge and the field reversal time. Thus, ζ_z(mid) is not expected to depend strongly on τ_I as Figure 12 demonstrates.

Summary

The motivation for this work was to better understand the TEB/TED behavior of short DNA fragments at electric field strengths that are large enough to distort the global conformation from its equilibrium (no field) value. In addition, we wanted to study the effects of field modulation on TEB/TED behavior in modeling studies since field modulation may eliminate some of the conformational distortion that occurs in a conventional TEB/TED experiment.[4] This was accomplished by carrying out Brownian dynamics simulations of a polyion modeled as a semiflexible string of beads. The most difficult aspect of this problem involves accounting for the interaction of the polyion with an external electric field. The ion atmosphere is not treated explicitly but rather implicitly by placing effective charges on the bead subunits which, in turn, interact with the external field. To model the effective charge component that arises from the polarization of the polyion in an external field, a stochastic "single lifetime" model based on the work of Szabo, Haleem, and Eden[22] is developed. Although characterizing the complex electrostatic interaction in terms of a three-parameter model (q_{sub}, polyion polarizability, and single ion atmosphere relaxation time) is a simplification of the problem, it should be adequate in predicting the qualitative features of an actual TEB/TED experiment.

The polyion of primary interest in this work is a 194 bp DNA fragment (modeled as a string of 10 beads) placed in an external field of 25 kV/cm since a fragment of this size exhibits distortion/amplitude inversion above a field strength of about 10 kV/cm[14] and has been considered in preliminary modeling studies.[18] In the absence of field modulation, we have demonstrated unequivocally that this polyion is deformed through bowing (caused by the translation of the polyion through a viscous fluid) and stretching (caused by charge polarization). Even in the limit of zero polarizability, some birefringence/dichroism is observed which is due to bowing. When the steady state dc field (turned on for a duration of 8 μs) is replaced with a rapidly reversing dc field (of period $2T'$), then the bowing deformation is largely eliminated provided T' is smaller than the coil-deformation times and T' is longer than the ion atmosphere relaxation time (τ_I). Under these conditions the TEB/TED decay is simplified and looks similar to that observed at much lower electric fields since deformations are largely reduced. This effect has been observed in some experiments on high molecular weight synthetic polyions.[4] Thus, one advantage of the field modulation technique in birefringence/dichroism is that it makes characterizing the equilibrium conformation of the polyion simpler and more straightforward by eliminating much of the deformation that arises when the polyion is subjected to an external field. It should be emphasized, however, that the deformations that arise from charge polarization are not eliminated. The response time of the ion atmosphere, τ_I, will influence the results of a field modulation experiment since when $\tau_I > T'$, there is insufficient time for the external field to orient the polyion before the field is reversed and hence the steady state birefringence/dichroism is reduced substantially. There appears to be very little experimental data on τ_I.[22] The field modulation method coupled with Brownian dynamics simulations similar to those presented in this work may provide a viable method of measuring these lifetimes.

References and Notes

(1) Vesterberg, O. *Electrophoresis* **1994**, *14*, 1243.

(2) Schwartz, D. C.; Cantor, C. R. *Cell* **1984**, *37*, 67.

(3) *Electrophoresis of Large DNA Molecules*; Lai, E., Birren, B. W., Eds.; Cold Springs Harbor Laboratory Press: Plainview, 1990.

(4) Oppermann, W. In *Colloid and Molecular Electro-Optics*, 1991; Jennings, B. K., Stoylov, S. P., Eds.; Institute of Physics: Bristol, 1992; p 93.

(5) Porschke, D. *Biophys. Chem.* **1994**, *51*, 37.

(6) Porschke, D. *Biophys. Chem.* **1994**, *49*, 127.

(7) Plum, G. E.; Bloomfield, V. A. *Biopolymers* **1990**, *29*, 1137.

(8) Antosiewicz, J.; Porschke, D. *J. Phys. Chem.* **1991**, *95*, 5983.

(9) Yamaoka, K.; Fukudome, K. J. *J. Phys. Chem.* **1988**, *92*, 4994.

(10) Yamaoka, K.; Fududome, K. J. *J. Phys. Chem.* **1990**, *94*, 6896.

(11) Elias, J. G.; Eden, D. *Macromolecules* **1981**, *14*, 410.

(12) Stellwagen, N. C. *Biopolymers* **1981**, *20*, 434.

(13) Hagerman, P. J. *Biopolymers* **1981**, *20*, 1503.

(14) Diekmann, S.; Hillen, W.; Morgeneyer, B.; Wells, R. D.; Porschke, D. *Biophys. Chem.* **1982**, *15*, 263.

(15) Lewis, R. J.; Allison, S. A.; Eden, D.; Pecora, R. *J. Chem. Phys.* **1988**, *89*, 2490.

(16) Allison, S. A.; Nambi, P. *Macromolecules* **1992**, *25*, 759.

(17) Antosiewicz, J.; Porschke, D. *Biophys. Chem.* **1989**, *33*, 19.

(18) Elvingson, C. *Biophys. Chem.* **1992**, *43*, 9.

(19) Allison, S. *Macromolecules* **1993**, *26*, 4715.

(20) Fixman, M.; Jagannathan, S. *J. Chem. Phys.* **1981**, *75*, 4048.

(21) Charney, E. *Quant. Rev. Biophys.* **1988**, *21*, 1.

(22) Szabo, A.; Haleem, M.; Eden, D. *J. Chem. Phys.* **1986**, *85*, 7472.

(23) Allison, S. A.; Sorlie, S. S.; Pecora, R. *Macromolecules* **1990**, *23*, 1110.

(24) Wu, P.; Fujimoto, B. S.; Schurr, J. M. *Biopolymers* **1987**, *26*, 1463.

(25) Provencher, S. W. *Comput. Phys. Commun.* **1982**, *27*, 213, 229.

(26) Manning, G. S. *Q. Rev. Biophys.* **1978**, *11*, 179.

(27) Smith, S. B.; Bendich, A. J. *Biopolymers* **1990**, *29*, 1167.

(28) Wesenberg, G. E.; Vaughan, W. E. *J. Chem. Phys.* **1987**, *87*, 4240.

(29) Ermak, D.; McCammon, J. A. *J. Chem. Phys.* **1978**, *69*, 1352.

(30) Rotne, J.; Prager, S. *J. Chem. Phys.* **1969**, *50*, 4831.

(31) Odijk, T. J. Polym. Phys. Ed. **1977**, *15*, 477.

(32) Skolnick, J.; Fixman, M. *Macromolecules* **1977**, *10*, 944.

(33) Schurr, J. M.; Allison, S. A. *Biopolymers* **1981**, *20*, 251.

(34) Allison, S. A.; Austin, R.; Hogan, M. *J. Chem. Phys.* **1989**, *90*, 3843.

(35) Mathews, J.; Walker, R. L. *Mathematical Methods of Physics*, 2nd ed.; W. A. Benjamin: Menlo Park, CA, 1970; p 408.

(36) Heath, P. J.; Allison, S. A.; Gebe, J. A.; Schurr, J. M. *Macromolecules* **1995**, *28*, 6600.

(37) Song, L.; Allison, S. A.; Schurr, J. M. *Biopolymers* **1990**, *29*, 1773.

(38) Grycuk, T.; Antosiewicz, J.; Porschke, D. *J. Phys. Chem.* **1994**, *98*, 10881.

(39) Wesenberg, G. E.; Vaughan, W. E. *Biophys. Chem.* **1983**, *18*, 381.